

Self-assembly and Solvatochromic Fiber Formation of 4,5-Bis(dodecylthio)tetrathiafulvalene-4'-carboxylic Acid and Its Derivatives

Hideo Enozawa, Youhei Honna, and Masahiko Iyoda*
 Department of Chemistry, Graduate School of Science and Engineering,
 Tokyo Metropolitan University, Hachioji, Tokyo 192-0397

(Received September 13, 2007; CL-071007; E-mail: iyoda@tmu.ac.jp)

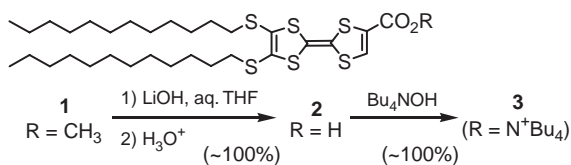
TTF-carboxylic acid **2** exhibits gelling ability for hexane and cyclohexane to form an orange fibrous material and shows solvatochromism both in solution and in the fiber formation to produce a reddish-purple fibrous material from acetonitrile. Moreover, the corresponding ester **1** forms yellow fibers from acetonitrile. However, the tetrabutylammonium salt **3** produces fine microcrystals without gel or fiber formation.

The synthetic chemistry of tetrathiafulvalenes (TTFs) has developed for the past 35 years,¹ and their attractive physical properties such as conductivity,² superconductivity,³ and magnetic properties⁴ have been extensively investigated by materials scientists. However, almost no attention has been paid to the self-assembling nanostructures, fiber, and other features of formation of TTFs except for the “fastner effect” of TTF derivatives with long alkyl chains.⁵ Recently, several groups have reported that TTFs and their oligomers form nanostructures such as nanofibers, nanotapes, and nanotubes.⁶ Moreover, we have shown the self-assembly of disc-like hexakis(tetrathiafulvalenyl-ethynyl)benzene resulting in pronounced stacking in solution and in the formation of a hexagonal fiber in solid state.⁷ The molecular framework of TTFs seems to be very effective for the formation of nanostructures.⁸ We report here either the self-assembly or solvatochromic fiber formation of simple TTF derivatives.

The methyl ester **1** and the carboxylic acid **2** were prepared from the corresponding TTF-diester by a modification of a reported procedure (Scheme 1).⁹ The tetrabutylammonium salt **3** was prepared by simply mixing **2** with an equimolar amount of Bu₄NOH in THF–methanol and then drying the mixture to remove solvents. The compounds **1–3** can be stored for a long time at 5 °C without decomposition.

The cyclic voltammetric (CV) analysis of **1** and **2** revealed fairly low oxidation potentials and hence good donor abilities; both **1** (5×10^{-3} M) and **2** (5×10^{-3} M) showed two reversible redox waves at 0.12 and 0.50 V and 0.10 and 0.47 V vs. Fc/Fc⁺, respectively.¹⁰ The first oxidation potentials of **1** and **2** are 0.20–0.18 V higher than that of TTF and comparable to that of BEDT-TTF ($E^1_{1/2} = 0.04$ V and $E^2_{1/2} = 0.37$ V vs. Fc/Fc⁺ under similar conditions).

The ¹H NMR and UV–vis spectra of **1** and **3** in CDCl₃



Scheme 1. Synthesis of 4,5-bis(dodecylthio)tetrathiafulvalene-4'-carboxylic ester **1** and its derivatives **2** and **3**.

showed no concentration dependence due to the lack of self-aggregation of these compounds in solution. As expected, **2** showed a monomer–dimer equilibrium in solution, and hence the ¹H NMR and UV–vis spectra of **2** showed a concentration dependence. Thus, the λ_{\max} of 0.00908 mM cyclohexane solution of **2** is 440 nm ($\epsilon = 1.99 \times 10^3$ M⁻¹ cm⁻¹), whereas that of 0.908 mM cyclohexane solution of **2** is 459 nm ($\epsilon = 2.18 \times 10^3$ M⁻¹ cm⁻¹). The red shift by 19 nm is due to the monomer–dimer equilibrium of **2** in cyclohexane.¹¹

Interestingly, **2** gelled hexane (>10 mg cm⁻³) and cyclohexane (>30 mg cm⁻³) at room temperature to produce a reddish-orange gel (Figure 1a). The microscopic image (Figure 1b) of xerogel of **2** shows a fine fibrous structure. However, **2** did not gelate CH₃CN but formed reddish-violet fibrous precipitate having a thicker-wire structure (Figure 1c). In the case of **1**, no gelation was observed for the common organic solvents, but a yellow fibrous material was formed from CH₃CN. The microscopic and SEM images (Figures 1d and 1e) of the fibrous material of **1** show a tape-like morphology of 2–10- μ m width and 100–1000-nm thickness. The ammonium salt **3** formed no gel or fibrous material from the common organic solvents and produced microcrystals from hexane, cyclohexane, or diisopropyl ether (Figure 1f). Although ionic amphiphilic systems often exhibit gel formation,^{7,12} the ammonium carboxylate **3** shows no gelation or fiber formation. Similarly, the corresponding lithium salt showed no gelation or fiber formation.

The XRD profile of **1** fiber showed a regular reflection pat-

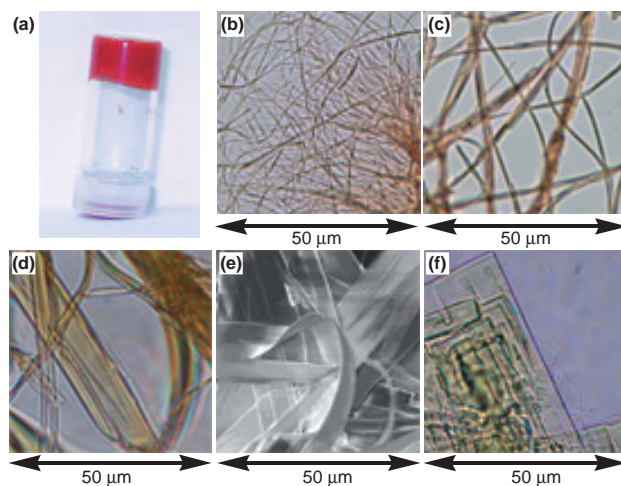


Figure 1. (a) Cyclohexane gel of **2**. (b) Optical micrograph of xerogel of **2**. (c) Optical micrograph of reddish-violet fibrous structure of **2**. (d) Optical micrograph of tape-like structure of **1** from CH₃CN. (e) SEM image of tape-like structure of **1**. (f) Microplates of **3** from cyclohexane.

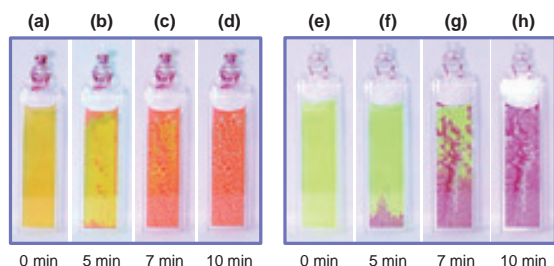


Figure 2. Solvatochromism of the TTF-carboxylic acid **2** in solution and the fibrous structure. (a)–(d) Fiber formation from hot hexane solution of **2** (2 mg cm^{-3}). (e)–(h) Fiber formation from hot CH_3CN solution of **2** (2 mg cm^{-3}).

tern and a distinct (100) peak at $2\theta = 2.05^\circ$ (4.31 nm) together with higher-order reflections observed in a small-angle region, indicating a considerably high crystallinity and the existence of a lamellar structure of 4.31-nm pitch.¹³ Since the molecular size of **1** was estimated to be ca. 28 Å, a dimeric structure with a stacked head-to-head or head-to-tail arrangement could be expected.

It is noteworthy that the colors of **2** fibers prepared from hexane and CH_3CN are quite different. Thus, **2** shows solvatochromism both in solution and in the fiber formation. As indicated in Figures 2a–2d, a hot dilute solution of **2** in hexane (2 mg cm^{-3}) was gradually cooled. First, a hot clear-orange solution (Figure 2a) showed UV–vis absorption at λ_{max} 456 nm. After 5 and 7 min, a reddish-orange fibrous material was gradually formed (Figures 2b and 2c), and the fiber formation was almost complete after 10 min (Figure 2d). The fibrous material showed UV–vis absorption at λ_{max} ca. 500 nm. In contrast, a hot dilute solution of **2** in CH_3CN exhibited a different behavior. A hot clear-yellow solution of **2** in CH_3CN (2 mg cm^{-3}) (Figure 2e) shows UV–vis absorption at λ_{max} 418 nm. After 5 and 7 min, a reddish-violet fibrous material was gradually formed (Figures 2f and 2g), and the fiber precipitation was almost complete after 10 min (Figure 2h). This fibrous material showed absorption at λ_{max} ca. 580 nm. SEM and AFM images showed that the reddish-orange fiber was of 50–500-nm width and 20–100-nm thickness and that the reddish violet fiber was of 1–2- μm width and 100–1000-nm thickness.¹⁴

The XRD profile of the reddish-orange fiber as shown in Figure 2d revealed a regular reflection pattern and a distinct (100) peak at $2\theta = 2.34^\circ$ (3.77 nm) together with higher-order reflections; The reddish-violet fiber (Figure 2h) showed a similar regular reflection pattern with a distinct (100) peak at $2\theta = 2.40^\circ$ (3.56 nm) and higher-order reflections.¹⁵ Thus, the XRD profiles of fibrous materials from hexane and CH_3CN indicate a fairly high crystallinity and lamellar structures of 3.77 and 3.56 nm, respectively. Since **2** forms a dimer in solid state, the size of the dimer is estimated to be ca. 5.6 nm. The alkyl–alkyl interaction in CH_3CN should be stronger than that in hexane and cyclohexane. Therefore, a stronger alkyl–alkyl overlap in a CH_3CN solution results in a shorter pitch of the lamellar structure, probably leading to a closer stacking of the TTF moiety. It is known that a J-type aggregation of chromophores results in a red shift, the lamellar structure prepared from a CH_3CN solution leads to a stronger face-to-face interdimer interaction of the TTF moiety. In summary, it is apparent that TTF-carboxylic acid and its derivatives with long alkylthio chains adopt various morphologies

depending on their functional substituent and the solvent employed.

This work was supported in part by a Grant-in-Aid for Scientific Research on Priority Areas of Molecular Conductors (No. 15073219) from the Ministry of Education, Culture, Sports, Science and Technology, Japan. We are grateful to Dr. Masashi Hasegawa and Dr. Tohru Nishinaga for helpful discussions.

This paper is dedicated to the memory of the Emeritus Professor Yoshihiko Ito of Kyoto University.

References and Notes

- 1 a) *TTF Chemistry*, ed. by J. Yamada, T. Sugimoto, Kodansha & Springer-Verlag, Tokyo, **2004**. b) J. Yamada, H. Akutsu, H. Nishikawa, K. Kikuchi, *Chem. Rev.* **2004**, *104*, 5057. c) M. Iyoda, M. Hasegawa, Y. Miyake, *Chem. Rev.* **2004**, *104*, 5085. d) J. O. Jeppesen, M. B. Nielsen, J. Becher, *Chem. Rev.* **2004**, *104*, 5115. e) J. M. Fabre, *Chem. Rev.* **2004**, *104*, 5133.
- 2 a) U. Geiser, J. A. Schlueter, *Chem. Rev.* **2004**, *104*, 5203. b) M. Fourmigué, P. Batail, *Chem. Rev.* **2004**, *104*, 5379; G. C. Papavassiliou, A. Terzis, P. Delhaes, in *Handbook of Organic Conductive Molecules and Polymers*, ed. by H. S. Nalwa, John Wiley & Sons: Chichester, **1997**, p. 151.
- 3 a) H. Kobayashi, H. Cui, A. Kobayashi, *Chem. Rev.* **2004**, *104*, 5265. b) R. P. Shibaeva, E. B. Yagubskii, *Chem. Rev.* **2004**, *104*, 5347. c) D. Jérôme, *Chem. Rev.* **2004**, *104*, 5565.
- 4 a) E. Coronado, P. Day, *Chem. Rev.* **2004**, *104*, 5419. b) T. Enoki, A. Miyazaki, *Chem. Rev.* **2004**, *104*, 5449.
- 5 H. Inokuchi, G. Saito, P. Wu, K. Seki, T. B. Tang, T. Mori, K. Imaeda, T. Enoki, Y. Higuchi, K. Inaka, N. Yasuoka, *Chem. Lett.* **1986**, 1263.
- 6 a) M. Jørgensen, K. Bechgaard, T. Bjørnholm, P. Sommer-Larsen, L. G. Hansen, K. Schaumburg, *J. Org. Chem.* **1994**, *59*, 5877. b) J. Sly, P. Kasák, E. Gomar-Nadal, C. Rovira, L. Górriz, P. Thorarson, D. B. Amabilino, A. E. Rowan, R. J. M. Nolte, *Chem. Commun.* **2005**, 1255. c) T. Akutagawa, K. Kakiuchi, T. Hasegawa, S. Noro, T. Nakamura, H. Hasegawa, S. Mashiko, J. Becher, *Angew. Chem., Int. Ed.* **2005**, *44*, 7283. d) T. Kitamura, S. Nakaso, N. Mizoshita, Y. Tochigi, T. Shimomura, M. Moriyama, K. Ito, T. Kato, *J. Am. Chem. Soc.* **2005**, *127*, 14769. e) T. Kitahara, M. Shirakawa, S. Kawano, U. Beginn, N. Fujita, S. Shinkai, *J. Am. Chem. Soc.* **2005**, *127*, 14980. f) C. Wang, D. Zhang, D. Zhu, *J. Am. Chem. Soc.* **2005**, *127*, 16372. g) H. Enozawa, M. Hasegawa, D. Takamatsu, K. Fukui, M. Iyoda, *Org. Lett.* **2006**, *8*, 1917.
- 7 M. Hasegawa, H. Enozawa, Y. Kawabata, M. Iyoda, *J. Am. Chem. Soc.* **2007**, *129*, 3072.
- 8 Y. Kobayashi, M. Hasegawa, H. Enozawa, M. Iyoda, *Chem. Lett.* **2007**, *36*, 720.
- 9 M. M. S. Abdel-Mottaleb, E. Gomar-Nadal, M. Surin, H. Uji-i, W. Mamdoui, J. Veciana, V. Lemaure, C. Rovira, J. Cornil, R. Lazzaroni, D. B. Amabilino, S. De Feyter, F. C. De Schryver, *J. Mater. Chem.* **2005**, *15*, 4601.
- 10 The cyclic voltammetric analysis was carried out under the following conditions: 0.1 M $\text{Bu}^n_4\text{NClO}_4$, CH_2Cl_2 , 100 mV s^{-1} , Pt working and counter electrodes, Ag/Ag^+ reference electrode, see Supporting Information which is available electronically on the CSJ-Journal Web site, <http://www.csj.jp/journals/chem-lett/>.
- 11 The monomer–dimer equilibrium was confirmed by vapor pressure osmometric (VPO) analysis, see Supporting Information.
- 12 F. J. M. Hoeben, P. Jonkheijm, E. W. Meijer, A. P. H. J. Schenning, *Chem. Rev.* **2005**, *105*, 1491.
- 13 For the XRD reflectogram of fibrous material of **1**, see Supporting Information.
- 14 For the SEM and AFM images of reddish-orange fiber and reddish-violet fiber, see Supporting Information.
- 15 For the XRD reflectograms of fibrous materials of **2**, see Supporting Information.